Geometric and electronic structure effects in polarized V *K*-edge absorption near-edge structure spectra of V_2O_5

O. Šipr and A. Šimůnek
Institute of Physics, Academy of Sciences of the Czech Republic, Cukrovarnická 10, 162 53 Praha 6, Czech Republic

S. Bocharov, Th. Kirchner, and G. Dräger
Fachbereich Physik der Martin-Luther-Universität Halle-Wittenberg, Friedemann-Bach-Platz 6, D-06108 Halle, Germany
(Received 21 April 1999)

Experimental and theoretical polarized V *K*-edge spectra of V_2O_5 are presented. By analyzing experimental spectra, we find that quadrupole transitions are significant, although not dominant at the pre-edge region. Real-space multiple-scattering calculation, relying on a non-self-consistent muffin-tin potential, can account for the basic polarizations trends and for peak heights and positions of the experimental spectra. However, important differences between theory and experiment occur for low-photoelectron energies. Lack of selfconsistency, muffin-tin form of the potential, and complex core-hole effects are identified as possible sources of this discrepancy. We argue that this deficiency of the theory would not get revealed if unpolarized spectra were investigated only. Cluster-size convergence of the calculated spectra is not uniform and it depends on the polarization. By performing model calculations we find, that deviations of the V_2O_5 structure from a perfect horizontal symmetry are much less significant for the shape of the spectrum than deviations from the vertical symmetry. For generating the distinct prepeak in the spectrum, which is polarized along the vertical axis, both short V-O bond length and deviations from inversion symmetry are crucial. The high-energy tail of the spectrum (photoelectron energies more that 30 eV) seems to be generated by scattering from more distant atoms. [S0163-1829(99)10843-9]

I. INTRODUCTION

X-ray absorption near-edge structure (XANES) spectroscopy has become a useful tool for investigating both electronic and geometric structure of condensed materials. Generally, most experimental spectra can be reproduced reasonably well by one-electron theory relying on one of few ''established'' calculating techniques — such as real-space multiple-scattering (RS-MS) method,[1,2] band-structure calculation,[3] or molecular-orbital formalism.[4,5] Challenges in XANES theory persist mainly in a proper description of the core hole and adjoining many-electron effects,[6–9] a well-founded *ab initio* treatment of the energy-dependent selfenergy,[10,11] an inclusion of non-muffin-tin contributions,[12–15] a tractable accounting for intra-atomic electron-electron interaction,[16] as well as in construction of a self-consistent scattering potential without the need to perform a full-scale band-structure calculation.[17–19] However, even a larger obstacle in a broader use of XANES spectroscopy in structural studies probably poses the lack of an intuitive interpretation of XANES spectra. That's the reason why a lot of effort was devoted recently to finding a connection between particular geometric and spectral patterns.[20–23] Most of the attention has been concentrated on the pre-edge structure so far.[24–26]

Vanadium pentoxide V_2O_5 is an example of a compound where problems with ''standard'' XANES calculations could be anticipated: It has quite a distorted losely packed crystal structure, hence the self-consistency in potential as well as non-muffin-tin effects may be important. It offers a variety of symmetry distortions — a feature that appears to be crucial in the pre-edge region.[27,28] Apart from that, V_2O_5 itself is a member of the highly interesting vanadium oxides family. Unlike its more famous relatives, such as VO_2 or V_2O_3, it does not exhibit the metal-insulator transition. However, V_2O_5 still hosts a number of interesting physical properties useful for many scientific and technological applications (such as catalysis, solid-state batteries, solar cells, electronic, and optical switches).[29]

Quite a large number of publications dealing with XANES spectra of V_2O_5 (as well as of other vanadium oxides) was published in the past. An extensive comparison of unpolarized vanadium *K*-edge spectra of various vanadium compounds was presented by Wong *et al.*[27] They pay particular attention to the trends in the dependence of the pre-edge fine structure on the local vanadium coordination. They conclude that the distinct pre-peak in the XANES spectrum of V_2O_5 originates from $1s \rightarrow 3d$ transitions, which are made dipole allowed if the full local octahedral O_h symmetry is decreased. Also they present convincing semiquantitative arguments in support of the idea that the pre-edge structure originates from states generated by a cage formed by central vanadium and few nearest-neighbor oxygens. They did not present any comparison with theoretical spectra, however.

Stizza *et al.*[30,31] performed the first V *K*-edge XANES calculations for V_2O_5. As they relied just on the very nearest neighborhood of vanadium, they were not able to reproduce finer XANES details. Nevertheless, their calculations correctly accounted for overall polarization dependence of V *K*-edge spectra of V_2O_5 gel.

Polarized near-edge structure of V_2O_5 crystal at the V *K*-edge was published by Cherkashenko *et al.*,[32] who com-

pared their measurements with calculated total density of states (DOS) available that time from the literature. Another RS-MS calculation of polarized V *K* spectra of V_2O_5 in the pre-edge region for cluster sizes up to 19 atoms was presented by Kraizman *et al.*[33] and by Kraizman and Novakovich.[34] Although their calculation reproduces the basic polarization trends fairly well, they cannot reproduce the detailed fine pre-edge structure for $\boldsymbol{\varepsilon} \| x$ and $\boldsymbol{\varepsilon} \| y$ polarizations accurately ($\boldsymbol{\varepsilon}$ is the polarization vector of the incoming radiation). Authors attribute this failure to core-hole and/or non-muffin-tin effects. The anomalously short V-O bond and large deviations from the perfect O_h symmetry are suggested to be key elements in formation of the sharp $\boldsymbol{\varepsilon} \| z$ prepeak.

Poumellec *et al.*[28] compared experimental polarized V *K*-edge spectra of a V_2O_5 crystal and gel and of a $VOPO_4 \cdot 2H_2O$ gel. In these compounds, the nearest coordination of vanadium is quite similar, while the long-range order differs. As the gross features of the three spectra look quite similar (especially close to the edge), it can be concluded that the most distinct structures in the XANES spectra of V_2O_5 are determined predominantly by multiple scattering within the first neighboring shell. It is suggested, that the weak prepeak appearing in case of a polarization vector lying inside the V-O layer (i.e., $\boldsymbol{\varepsilon} \| x,y$) is partially formed by a quadrupole transition. The role of symmetry distortions from the perfect O_h square bipyramid for the intensity of pre-edge peaks is stressed.[28] In a recent publication,[35] polarized V *K*-edge XANES of $VOPO_4 \cdot 2H_2O$ gel was measured and calculated and quadrupole contributions at the pre-edge region were identified.

Polarized V L_3-edge and O *K*-edge XANES spectra were measured and compared with DOS obtained from linear combination of atomic orbitals (LCAO) calculation.[36] The theory accounts correctly for the basic trends in polarization dependence, however, the detailed spectral features are reproduced not very accurately. Unoccupied states of V_2O_5 reaching up to 6 eV above the edge were investigated via band-structure technique (augmented spherical wave method) by Eyert and Höck.[37] They concentrated on the effect of symmetry distortions on both occupied and unoccupied electron states. Partial V 3*d* DOS they obtain compares with V L_3-edge XANES spectra considerably better than the LCAO results.[36] It seems thus probable that deviations between theory and experiment apparent in Ref. 36 are rather caused by deficiencies of the LCAO method itself than, e.g., by neglect of intra-atomic electron-electron interactions.[16]

The purpose of our paper is to elucidate further the interplay between the real and the electronic structure in the formation of XANES spectra. By investigating polarized spectra of a loosely packed semilayered V_2O_5, the calculations are especially sensitive to the details of scattering potential construction. The local coordination of V atom (distorted octahedron) provides an opportunity to study the much debated effects of symmetry distortion on the pre-edge fine structure in a systematic way — by comparing theoretical spectra for various model compounds. Also we intend to pay attention to the whole XANES region (i.e., not only prepeak), as in such a case more features are offered for comparison between experiment and theory, providing thus possibility to set accountable limits on the reliability of the conclusions. Effects of clusters larger than studied so far[31,33] should also be investigated. The question of significance of quadrupole transitions at the pre-edge seems ought to be studied, too.

TABLE I. Positions of the vanadium atoms and of the three types of oxygens in the V_2O_5 crystal.

Original V_2O_5 structure				
Atom	Wyckoff positions	*x*	*y*	*z*
V	(4f)	0.10118	0.25	0.8917
O_{van}	(4f)	0.1043	0.25	0.531
O_{ch}	(4f)	−0.0689	0.25	0.003
O_{bri}	(2a)	0.25	0.25	0.001

The plan of our paper is as follows: First, we describe the structure of V_2O_5 with particular emphasis on the vanadium neighborhood. Then, we describe the experimental settings and the procedure used to obtain individual polarization components. Specific aspects of our calculation method are outlined in Sec. III. In the discussion (Sec. IV) we compare the theory with experiment, investigate effect of changing some parameters that determine the muffin-tin potential on the resulting spectra, and estimate the role of quadrupole transitions. The substantial part of the discussion is devoted to the effects of changing the symmetry of the whole crystal and to the role of particular atoms in vanadium neighborhood for the XANES spectra.

II. EXPERIMENT

A. V_2O_5 crystal structure

Vanadium pentoxide V_2O_5 crystallizes in the space group *Pmmn* (D_{2h}^{13}, No. 59). Orthorhombic lattice constants are $a = 11.512$, $b = 3.564$, and $c = 4.368$ Å . Positions of the vanadium atoms and of the three types of oxygens — vanadyl (O_{van}), chain (O_{ch}) and bridge (O_{bri}) — are given in fractional units in Table I. The nearest neighborhood of the vanadium atom forms a highly distorted bipyramid (see Fig. 1). In the ''horizontal'' *ab* plane, the chains formed by the oxygen atoms O_{ch} are distorted from the straight line (Fig. 2). There is also a ''vertical'' symmetry distortion: Apart from

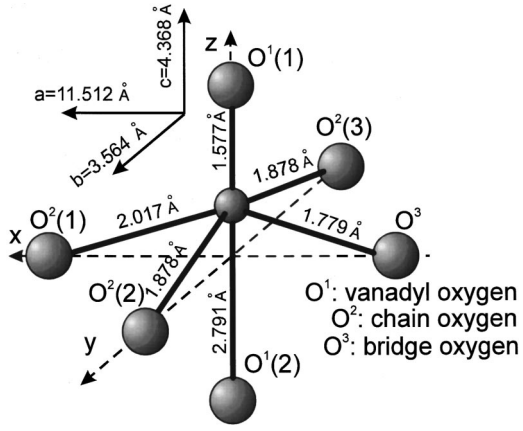

FIG. 1. Local coordination of a vanadium atom in V_2O_5. Indicated are also crystal axes and nearest-neighbor distances. The vanadium atom is in the center.

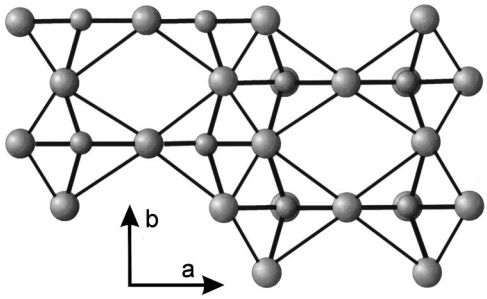

FIG. 2. Schematic depiction of the crystal structure of V_2O_5. A horizontal distortion of V–O chains in the y direction is demonstrated by projecting the V_2O_5 structure on its ab plane. Small balls stand for vanadiums and large balls for oxygens.

the obvious asymmetry of the vanadyl oxygens O_{van}, the atoms forming the pyramidal basis are not all in the same plane (Fig. 3).

B. Samples and measurements

The absorption sample was prepared by splitting a plate of some 10-μm thickness from a V_2O_5 single crystal. The plate was placed on a standard lead holder with the effective diaphragm diameter of 2 mm.

Our experimental setting is shown schematically in Fig. 4. In the starting position, the crystal axis c was parallel to the beam direction $\boldsymbol{k}$, and the axis a was parallel to the polarization vector $\boldsymbol{\varepsilon}$. Any orientation of the sample with respect to the vectors $\boldsymbol{\varepsilon}$ and $\boldsymbol{k}$ could be set through rotations in a PC-controlled goniometer around three perpendicular axes (denoted ψ, θ and ϕ in Fig. 4).

For the polarization dependent XANES measurements, the facilities of the synchrotron beamline E4 at HASYLAB (DESY) were used. Its performance in the energy region of V K-edge reaches 1.0×10^{10} photons/sec/mm^2 for the photon flux at the sample, and about 1.8 eV for the energy resolution. Ionic chambers were applied for detection of x-ray intensities.

C. Symmetry decomposition

For the polarization analysis we used a technique described in Refs. 38 and 39. Here, we only remind, that for the

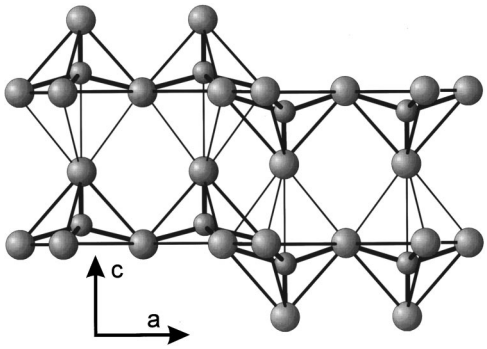

FIG. 3. Schematic depiction of the crystal structure of V_2O_5. A vertical distortion of the V-O planes is demonstrated by projecting the V_2O_5 structure on the ac plane. Small balls stand for vanadiums and large balls for oxygens.

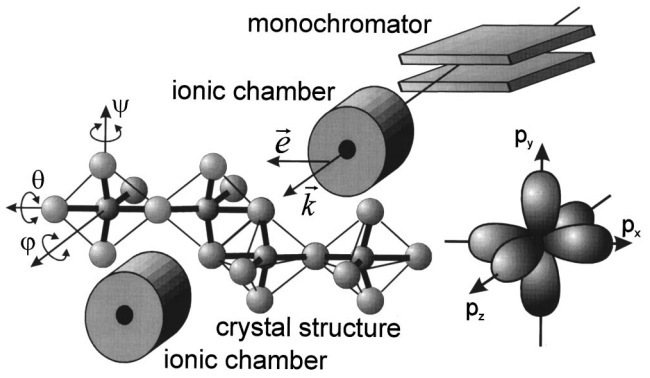

FIG. 4. The experimental apparatus scheme. The polarization vector $\boldsymbol{\varepsilon}$ and the wave vector $\boldsymbol{k}$ of the incoming radiation as well as the orientation of the V_2O_5 crystal with respect to this beam are shown. See Sec. II C for further description.

K-edge the total absorption μ can be described as a linear combination of partial symmetry resolved spectral components, viz. p_x, p_y, p_z for dipole transitions and d_{xy}, d_{yz}, d_{xz}, $d_{x^2-y^2}$, d_{z^2} for quadrupole transitions:

$$\mu=\mu_D+\mu_Q,$$

$$\mu_D\propto p_x\varepsilon_x^2+p_y\varepsilon_y^2+p_z\varepsilon_z^2, \tag{1}$$

$$\begin{aligned}\mu_Q\propto{}& d_{xy}(\varepsilon_xk_y+\varepsilon_yk_x)^2+d_{xz}(\varepsilon_xk_z+\varepsilon_zk_x)^2\\ &+d_{yz}(\varepsilon_yk_z+\varepsilon_zk_y)^2+d_{x^2-y^2}(\varepsilon_xk_x+\varepsilon_yk_y)^2\\ &+\sqrt{3}d_{z^2}(\varepsilon_zk_z)^2.\end{aligned} \tag{2}$$

The symmetry resolved components originate from electron transitions between an inner $1s$ state and outer states of definite angular symmetry. The weight of each of the symmetry resolved components depends only on the positions of the polarization and wave vectors $\boldsymbol{\varepsilon}$ and $\boldsymbol{k}$ of the absorbed x-ray quantum with respect to the symmetry axes of the orbitals. These geometrical orientations, and consequently the spectral weights of the components, are defined by the coordinates of the vectors $\boldsymbol{\varepsilon}$ and $\boldsymbol{k}$ in the coordinate system of those electron orbitals, which are involved in the K absorption process [Eqs. (1)–(2)].

Although the dipole approximation has been generally accepted as well founded in XANES calculations, the question of quadrupole transitions is frequently raised when discussing the prepeak region. A convincing demonstration of presence of quadrupole transitions based on their angular dependence[40] was presented for a complex crystal containing a $CuCl_4^{2-}$ planar unit.[41] Another compound, for which quadrupole transitions were reported, is TiO_2 rutile crystal.[14,42] Detectable contributions of quadrupole components were clearly established also for $FeCO_3$ (Ref. 43) and for NiO and FeO (Ref. 44). Recently quadrupole transitions were identified in V K-edge XANES of $VOPO_4\cdot2H_2O$ gel.[35] As this compound is both structurally and chemically similar to V_2O_5, it is reasonable to expect that quadrupole transitions might be nonnegligible for the latter compound as well.

On general grounds, quadrupole transitions in the V K-edge absorption spectra of V_2O_5 can be expected to have intensities at least by an order weaker than the dipole ones.

One way of identifying them is to calculate dipole partial spectral components p_x, p_y, and p_z from Eq. (1), neglecting all the *d* components. If quadrupole transitions were absent, the *p* spectral components calculated from different sets of measured spectra would be the same. Hence, if appropriate *p* components do not coincide in a particular energy region, a non-negligible quadrupole contribution can be assumed.

Another way to visualize and estimate the quadrupole contribution is to exploit different polarization dependence of dipole and quadrupole spectral components.[39,41] Relying on Eqs. (1)–(2), one can select a group of such sample orientations, where all the *p* components have identical spectral weights, while the weights of the *d* components differ. The spread between the curves belonging to the same group then can arise from different quadrupole contributions only.

Both ways of identifying quadrupole transitions were used in our study (Sec. IV C).

III. THEORY

A. Construction of scattering potential

Polarized V *K*-edge XANES spectra of V_2O_5 were calculated employing the real-space multiple-scattering (RS-MS) formalism using the extensively revised ICXANES computer code of Vvedensky *et al.*[45] The largest angular momentum included in the single-site scattering was $l_{max}=4$ (this limit was checked for convergence). Coordinations of atoms in finite clusters of V_2O_5 atoms were generated with help of the CRYSTIN crystallographic database[46] and the PICTUR code of M. Dušek.[47]

The RS-MS approach relies on the so-called muffin-tin approximation, which considers the crystal potential to be spherically symmetric inside nonintersecting spheres around individual atoms and constant in the interstitial region. A non-self-consistent muffin-tin potential was generated via the so-called Mattheiss prescription:[48] Electron densities calculated for free atoms are put in appropriate positions of the crystal lattice, and coulombic and exchange parts of the crystal potential are calculated as superpositions of partial contributions from individual atoms. Electron densities for free atoms were calculated selfconsistently within the local density approximation by the LDAT code of J. Vackář.[49] The exchange-correlation potential of Ceperley and Adler[50] was used for atomic calculations of the occupied states. In constructing the Mattheiss potential appropriate for unoccupied states, the energy-independent $X\alpha$ potential with the Kohn-Sham value of $\alpha=0.66$ was used.[51] We do not employ energy-dependent exchange-correlation potential here as no universal recipe how to select its optimal form for a particular case has been known so far.[10,11]

Employing muffin-tin approximation invokes the need to set a few *ad hoc* parameters, which further specify the model — viz. the muffin-tin radii and the way of constructing the muffin-tin zero. As the muffin-tin approximation is an artificial concept, the final results ought not to depend ''too much'' on how these parameters are chosen. The opposite case would signal the breakdown of the muffin-tin approximation itself for the problem under study.

TABLE II. Muffin-tin radii R_{mft} in angstroms for each atomic type used in XANES calculations. The first parameter set corresponds to matching potential radii and interstitially averaged muffin-tin zero, the second set to matching potential radii and potential discontinuity minimizing muffin-tin zero and the third one to muffin-tin radii of Ref. 37 and interstitially averaged muffin-tin zero.

	V	O_{van}	O_{ch}	O_{bri}
Set 1, 2	0.893	0.683	0.807	0.751
Set 3	1.040	0.805	1.100	0.889

1. Parameters of muffin-tin potential

In the case of V_2O_5, insufficiency of muffin-tin approximation could be anticipated. Hence, we chose to test three modes of the muffin-tin potential: (1) Nonoverlapping muffin-tin radii were set so that the ''matching potential condition'' is satisfied and muffin-tin zero was identified with the proper average of the interstitial potential,[4] (2) muffin-tin radii were kept at the same values as in the previous case but the muffin-tin zero was identified with the inner-sphere potential at the muffin-tin radius of the O_{ch} atom, so that the overall discontinuity at muffin-tin boundaries is decreased,[52] and finally, (3) overlapping muffin-tin radii were taken the same as in the augmented spherical wave method study of V_2O_5 of Eyert and Höck[37] and the muffin-tin zero was constructed by interstitial averaging as in case (1). Thus, it turns out that the potentials corresponding to the parameter set 1 and set 2 are identical, except that the inner-sphere part of latter one is uniformly shifted by 7 eV upwards. Table II summarizes the muffin-tin radii for all three parameter sets.

2. Core-hole treatment

Proper incorporation of the core-hole left behind by the excited photoelectron poses quite a difficult—still not fully solved—task. To assess the importance of the core-hole effect, we calculated the XANES spectra both with and without the 1*s* core hole. We took the core hole into account while calculating atomic charge densities, by removing one electron from the V 1*s* level and putting it into its lowest unoccupied atomic level (''relaxed and screened'' model, practically equivalent to the frequently used $Z+1$approximation). Thus, the electronic configurations of the V atoms were $1s^2 \ldots 3d^3 4s^2$ for the ground state, and $1s^1 \ldots 3d^4 4s^2$ if the core hole was included. As plausible results obtained for a partially screened core-hole potential were reported for similar compounds as V_2O_5 (Refs. 35 and 53), we tested it as well (putting only a fractional charge *Q* into the lowest unoccupied vanadium orbital —''relaxed and partially screened'' model). The central V atom has a configuration $1s^1 \ldots 3d^{3+Q} 4s^2$ in such a case.

B. Quadrupole transitions

Quadrupole transtions (i.e., transitions to the *d* states) were included in our XANES calculation, too. Only ''technical'' modifications of the method with respect to the dipole-only case have to be considered. All the necessary

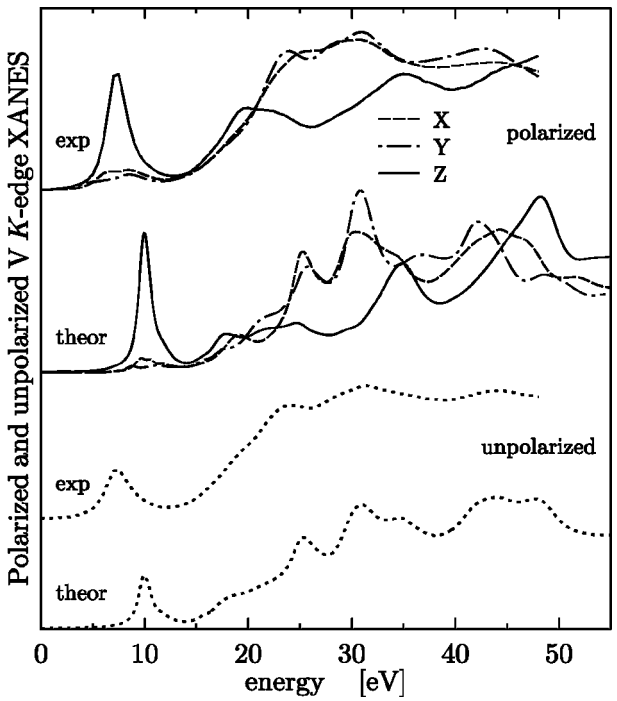

FIG. 5. Comparison of experimental and theoretical V *K*-edge XANES spectra of V_2O_5, both polarized and unpolarized. The polarized experimental components were obtained from several sets of measured polarized spectra, by procedure described in Sec. II C. The unpolarized experiment was obtained by averaging the polarized spectra. Theoretical curves correspond to the ''standard setting'' of potential parameters, as specified in the end of part III.

equations can be found, e.g., in Ref. 40. The results obtained by taking quadrupole contributions into account are presented in Sec. IV C.

Unless specified otherwise, all the theoretical curves presented here were calculated for a cluster of 119 atoms, with muffin-tin radii found by satisfying the matching potential condition and muffin-tin zero calculated as proper average of the potential in the interstitial region (parameter set 1 in Table II), employing the fully screened and relaxed core-hole potential, and involving dipole transitions only. Furthermore, unless explicitly stated otherwise, all theoretical results presented here include the convolution with a Lorentzian function, to take into account the lifetime of the 1*s* core hole of vanadium (full width at half maximum taken 1.01 eV, according to the compilation of Al Shamma *et al.*[54]).

IV. RESULTS AND DISCUSSION

A. Comparing theory and experiment

We summarize our basic experimental and theoretical spectra in Fig. 5. The partial spectral components of the experimental spectrum were obtained by procedure outlined in Sec. II C, neglecting possible quadrupole contributions (they will be handled separately when discussing the prepeak in Sec. IV C). Unpolarized experimental curve was obtained by averaging the three polarized components.

The zero of the energy scale was chosen by convenience. The experimental and theoretical spectra were aligned in the horizontal axis, so that the energy positions of the $\boldsymbol{\varepsilon}\|z$ peaks at $\sim$35 eV coincide. After such an alignment, the zero of our energy scale corresponds to the incident x-ray beam energy of 5462 eV for the experimental spectra.

Our transmission-mode measured polarized spectra are in a very good agreement with the spectra presented by Poumellec *et al.*,[28] which were obtained by total electron yield detection. An interesting difference can be observed at the double peak around 19–23 eV in $\boldsymbol{\varepsilon}\|z$ spectra: While the first subpeak (at 19 eV) is higher than the second one (at 23 eV) in Fig. 5, Poumellec *et al.*[28] observed an inverted ratio of these intensities (cf. Fig. 4 of their paper). It is not clear whether this is caused by different detection techniques or by something else. Note also that, in the preedge region, a good overall agreement with results of Cherkashenko *et al.*[32] occurs as well (their spectra do not exhibit sufficient resolution for higher energies). However, neither our spectra nor the spectra of Poumellec *et al.*[28] show the distinct kink on the high-energy side of the pre-peak in $\boldsymbol{\varepsilon}\|z$ observed in Ref. 32 — this feature is probably not a real effect.

Vanadium *K* spectra of V_2O_5 display a much larger polarization effect than the L_3 spectra: Goering *et al.*[36] did not find any difference between the $\boldsymbol{\varepsilon}\|x$ and $\boldsymbol{\varepsilon}\|y$ components and also the difference between any of the in-plane polarizations and the $\boldsymbol{\varepsilon}\|z$ component is much less pronounced at the L_3 edge. This can be understood intuitively realizing that L_3 spectra reflect mainly the density of the *d* states around vanadium, which bear more atomic character than the *p* states. Successful calculations of L_3-edge spectra of some transition metal compounds based on crystal-field split atomic multiplets[16] indicates that intra-atomic effects may indeed dominate in such a case. On the other hand, *K* spectra are more prone to solid-state effects (energy band dispersion).

As can be inferred from Fig. 5, our calculation describes well basic trends of the polarized spectra. Note that the position of the last peak in our $\boldsymbol{\varepsilon}\|z$ theoretical spectrum, which reaches beyond the range of our experiment, agrees well in position with the appropriate experimental peak of Ref. 28.

The energy separation between the prepeak and the main peak is smaller in theory than in experiment for any polarization. This is almost surely caused by the neglect of the energy-dependence of the selfenergy in our calculation.

The shoulders predicted by theory for the $\boldsymbol{\varepsilon}\|x$ component at 24 eV and for $\boldsymbol{\varepsilon}\|y$ at 21 eV do not have experimental counterparts. This may be due to effective smearing caused by inelastic losses of the photoelectron. Such processes are beyond the scope of our paper (our theoretical curves include just the core hole smearing).

The theory is not quite accurate for the $\boldsymbol{\varepsilon}\|z$ polarization at $\sim$20 eV — the theoretical peak is too wide: It stretches from 17 eV to 25 eV while the experimental structure stretches from 19 eV to 23 eV (Fig. 5). Furthermore, the theory also fails to reproduce correctly the polarization dependence of the $\boldsymbol{\varepsilon}\|x$ and $\boldsymbol{\varepsilon}\|y$ experimental peaks around $\sim$25 eV: Calculations predicts that the $\boldsymbol{\varepsilon}\|x$ maximum is lower in energy than the $\boldsymbol{\varepsilon}\|y$ maximum (at 25 eV and at 26 eV, respectively), while in experiment the $\boldsymbol{\varepsilon}\|y$ peak occurs for lower energy (at 23 eV) than the $\boldsymbol{\varepsilon}\|x$ peak (at 25 eV). One possible explanation at hand for this disagreement may be many-electron effects: Shakedown phenomena as the cause of the shoulder at the low-energy tail of the main peak were suggested by Ref. 27 for vanadium oxides or by Ref. 55 for copper complexes. Similarly, Curelaru *et al.*[56] argue on the basis of

comparing appearance potential, x-ray photoemission, x-ray emission, and x-ray absorption spectra, and diagram of molecular orbitals that the one-particle model of V_2O_5 spectra breaks down close to the edges. Although we cannot rule the many-electron option out, we would rather attribute the inaccuracies of our theory to the lack of selfconsistency and/or to the muffin-tin form of our scattering potential (cf. Sec. IV B 1).

The calculation does not reproduce correctly the pre-edge structure for $\boldsymbol{\varepsilon}\|x$ and $\boldsymbol{\varepsilon}\|y$ polarizations (similarly as Refs. 33 and 34). As demonstrated in Sec. IV C, this disagreement cannot be removed by merely including quadrupole contributions. The cluster size we used is fully sufficient, too (Sec. IV D). Again, the deficiency of our non-self-consistent potential can be the main source of this disagreement. However, the pre-edge structure is also quite sensitive to core-hole effects (Sec. IV B 2). Hence the inadequacy of our static ''$Z+1$''-like treatment of the core hole may contribute as well.

An interesting feature to note is that the comparison between the theory and the experiment looks significantly better for unpolarized spectra (lower curves in Fig. 5). This demonstrates that unpolarized spectra are ''more forgiving'' to deficiencies of the theory than polarized ones. Polarized spectra pose much more stringent test for any theory.

B. Choice of scattering potential

1. Different ways of constructing muffin-tin potential

As outlined in Sec. III A and summarized in Table II, we tested three ways of setting the ''defining parameters'' of the scattering potential. The results are displayed in Fig. 6. It can be seen, that although the gross features of the theoretical spectra do not depend on the particular choice of the muffin-tin parameters, the same is not true for some distinct details. Especially this is true in the pre-edge region. Neither choice of muffin-tin parameters leads to an essentially better reproduction of the experiment than the other two sets over the whole energy range. Interestingly, the frequently used way of constructing muffin-tin zero by minimizing the potential discontinuities at muffin-tin boundaries (parameter set 2) leads to the worst agreement between the theoretical and the experimental distance between the prepeak and main peak in the $\boldsymbol{\varepsilon}\|z$ component. This may of course change if energy-dependent selfenergy is employed. Note also that muffin-tin radii are usually set otherwise than by the matching potential method in case that a ''step-minimizing'' muffin-tin zero is used.[52] Hence, our study cannot strictly be taken as a test of which of the commonly used potential constructions is the best one.

The conclusion to be drawn from Fig. 6 is that certain details of V_2O_5 spectra are quite sensitive to the way of muffin-tin potential construction, and therefore their correct reproduction may require inclusion of non-muffin-tin effects.

2. Core-hole effect

We investigated the core-hole effect as well. We found hardly any difference between theoretical spectra calculated with a fully screened relaxed core hole and without it for $E > 15$ eV. The separation between the prepeak and the main peaks at $E \approx 25$ eV in the theoretical spectrum changes albeit not too much: It is by 1 eV smaller if the core hole is omitted.

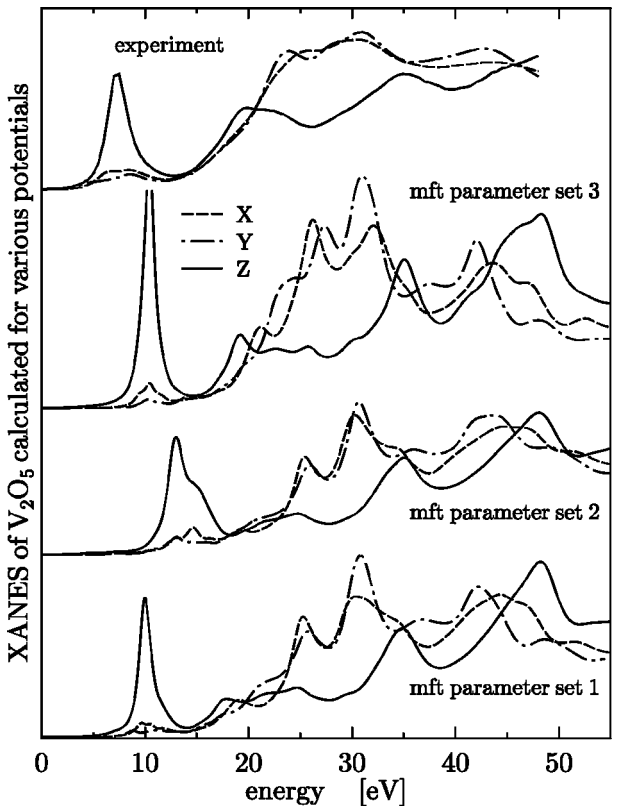

FIG. 6. Comparison of theoretical V *K*-edge spectra of V_2O_5 calculated for different sets of muffin-tin parameters, as specified in Table II: Matching-potential muffin-tin radii and interstitial averaged muffin-tin zero (lowest set of curves), matching-potential muffin-tin radii and potential step minimizing muffin-tin zero (middle set) and Eyert and Höck (Ref. 7) muffin-tin radii and interstitial averaged muffin-tin zero (uppermost theoretical set). Experimental spectrum is added at the top for comparison.

On the contrary, remarkable changes due to the core hole occur in the *preedge region*, as demonstrated in Fig. 7. The core hole effect depends quite a lot on the polarization: While it is very strong for the $\boldsymbol{\varepsilon}\|x$ and $\boldsymbol{\varepsilon}\|y$ polarizations, the $\boldsymbol{\varepsilon}\|z$ pre-peak is only mildly effected. A careful analysis of the raw — nonsmeared — theoretical data (depicted by broken curves in Fig. 7, cf. also bottom of Sec. III A) shows that the $\boldsymbol{\varepsilon}\|z$ pre-edge structure is in fact sensitive to the core-hole presence, too. However, the pre-edge structure obtained after smearing the raw $\boldsymbol{\varepsilon}\|z$ curve is dominated just by a single huge resonance at 10 eV, which itself does not depend on the presence or absence of the core hole. This resonance effectively overrides any other—core-hole-dependent—fine structure.

A plausible reason why this dominating resonance is not sensitive to the core-hole potential, is that this resonance is connected rather with the real than with the electronic structure of V_2O_5: As it will be explained below (Sec. IV F), this feature arises due to a very short and ''unilateral'' (i.e., not centrosymmetrical) $V-O_{van}$ bond. The rest of the pre-edge fine structure depends, on the other hand, quite a lot on the electronic structure due to the low-photoelectron energy, and hence, is quite prone to changes induced by the core hole.

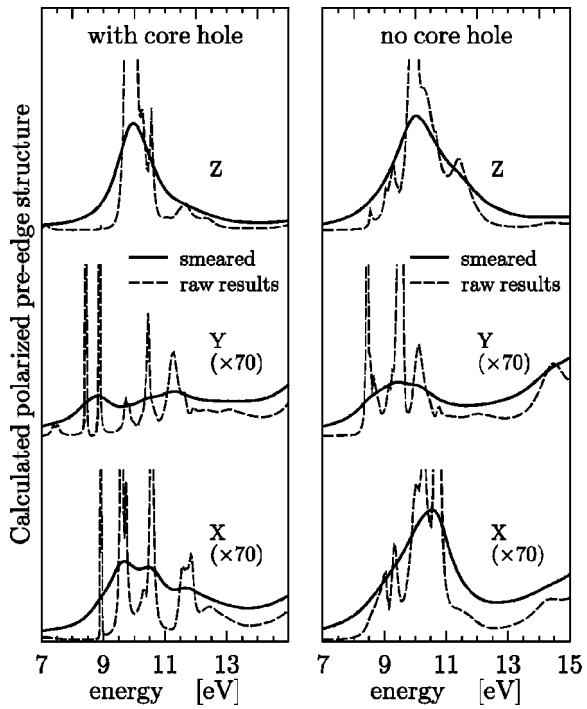

FIG. 7. Comparing polarized *theoretical* spectra in the pre-edge region obtained for potentials either including (left panel) or ignoring (right panel) the core hole. Thin dashed lines represent raw theoretical results, thick solid lines stand for curves broadened by convolution with lorentzians to account for finite core hole lifetime. The vertical scale is not the same for all polarizations — $\boldsymbol{\varepsilon}\|x$ and $\boldsymbol{\varepsilon}\|y$ component intensities were multiplied by 70 in order to be displayed together with the $\boldsymbol{\varepsilon}\|z$ component.

Thus, the apparent reason for the peculiar polarization-dependence of the core-hole effect rests in different mechanism of the pre-edge structure for the $\boldsymbol{\varepsilon}\|x,y$, and $\boldsymbol{\varepsilon}\|z$ polarizations.

The agreement with the experiment is quite poor in the $\boldsymbol{\varepsilon}\|x$ and $\boldsymbol{\varepsilon}\|y$ pre-edge regions, no matter whether the core hole is taken into account or not. Taking quadrupole transitions into account does not improve this agreement either (see Sec. IV C below). Nevertheless, we consider our theoretical models relevant enough to conclude that the core-hole effect might be quite significant at the $\boldsymbol{\varepsilon}\|x,y$ pre-edge. Unfortunately, it is not possible to attribute the failure of the theory in this region unambiguously either to deficiency of non-self-consistent potential, or to non-muffin-tin effects, or to inadequate ''$Z+1$'' treatment of the core hole. Let's just note that problems with incorporating the core hole into the V_2O_5 XANES calculation were reported earlier as well.[34]

We tried also a *partially screened* relaxed core hole potential, which was assessed as the most suitable one in earlier studies of $VOPO_4 \cdot 2H_2O$ (Ref. 35) and of other materials containing transition-metal atoms in distorted octahedral coordinations.[53] The screening charge Q varied in our tests from 0.2 to 0.8 of electron charge (as opposed to 1.0 in the case of a fully screened hole discussed above). We found that partial screening not only did not improve the agreement between theory and experiment in the pre-edge region, but even worsened it in the $E>15$ eV region. A possible cause of the apparent contradiction between our results and conclusions of Vedrinskii *et al.*[53] and Poumellec *et al.*[35] might rest in different ways of muffin-tin potential construction in their works.

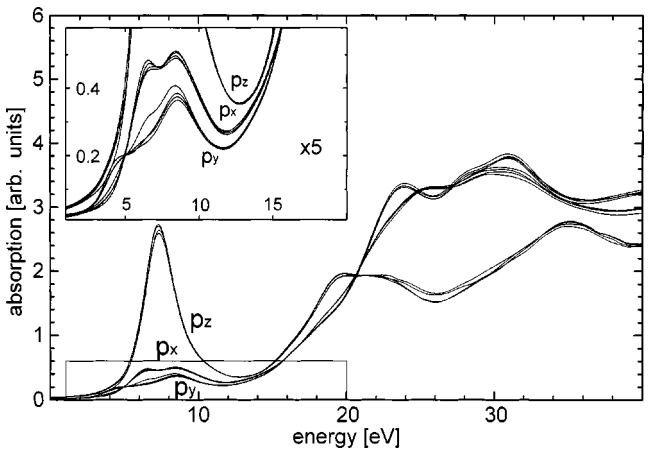

FIG. 8. Symmetry-resolved partial spectral components p_x, p_y, and p_z, extracted from four different sets of measured spectra. Possible quadrupole contributions were ignored. The vertical scale was expanded five times in the inset.

Finally, let us note that an *unpolarized spectrum* would not reveal any core-hole effect in the theory at all. The $\boldsymbol{\varepsilon}\|z$ prepeak, which is stable against the presence or absence of a core hole, presents namely by far the most dominant contribution to the unpolarized pre-peak (Fig. 5). Thus, any manifestation of significant changes in the $\boldsymbol{\varepsilon}\|x$ and $\boldsymbol{\varepsilon}\|y$ pre-edge structure, which are apparent in Fig. 7, would be obscured by the robust $\boldsymbol{\varepsilon}\|z$ component in the unpolarized spectrum.

C. Quadrupole transitions

States at the bottom of the conduction band of transition-metal compounds prevalently have a *d* character. Our RS-MS cluster calculation showed that the *d* DOS is about 100 times higher than the *p* DOS in the pre-edge region (we do not show the plots here for brevity). This overwhelming dominance of the *d* states makes another case for looking for quadrupole contributions.

First, let's review the experimental evidence based on methods described in Sec. II C. In Fig. 8, we present the partial spectra components p_x, p_y, and p_z extracted from four different sets of experimental spectra along Eq. (1), neglecting the quadrupole contributions. A good coincidence between the corresponding curves confirms the dipole character of the polarization dependence for energies above ~ 12 eV. At the same time, a quadrupole contribution is observed in the pre-edge region, below 12 eV (inset of Fig. 8). It should not be confusing, that at higher energies (above 15 eV) the absolute differences between the curves of the same polarization become even larger than in the pre-edge region. This happens because of the background fit error (growing with energy) and a possible imaginary decrease of absorption at its high values because of the so called thickness effect. The decisive factor here is, however, the relative spread, which anyway is much larger below 12 eV. The averaged experimental curves for p_x, p_y, and p_z are displayed in Fig. 5 at the top.

Another way of identificating quadrupole contributions is employed in Fig. 9: We display here experimental curves

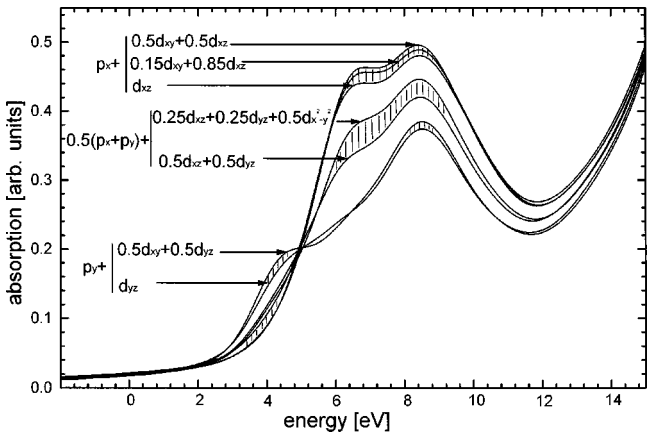

FIG. 9. Experimental V *K*-edge XANES curves recorded at selected sample orientations such that partial spectra weights of the *p* orbitals are identical while weights of the *d* orbitals vary. Partial spectral weights of the *p* and *d* components are indicated for each curve in the plot.

recorded at such sample-to-beam orientations that dipole spectral weights are identical, while quadrupole spectral weights differ. The partial spectral weights for each group are indicated in the plot.

Again, one can establish that the region of effective quadrupole contribution ends at 12 eV in our scale (note that our zero corresponds to 5462 eV of photon energy, as stated in Sec. IV A). The magnitude of spread indicates the strength of the quadrupole transition. Analyzing the weights of *p* and *d* components in each spectrum, one can see that in the middle group of spectra in Fig. 9, the component $d_{x^2-y^2}$ seems to be responsible for the increased absorption. Analogously, in the upper group, the component d_{xy} increases the absorption, while the component d_{xz} is evidently smaller (it decreases the peak intensity). Finally, from the lowest group one can conclude that the component d_{xy} is larger than d_{yz}. Thus, from all three groups it follows that the components d_{xy} and $d_{x^2-y^2}$ contribute to the pre-edge absorption, while d_{xz} and d_{yz} partial spectral components are comparatively small.

This observation is somewhat surprising, as selfconsistent band-structure calculations[37] show that the local density of the $d_{x^2-y^2}$ states is significantly smaller than local densities of either d_{xz} or d_{yz} states at the V site (see Fig. 6 of Ref. 37). Note however that x-ray absorption spectrum is not a *direct* probe of partial DOS (matrix elements play a role as well), so our finding need not be at variance with Ref. 37.

We took the quadrupole transitions into account in our theoretical calculations as well. Theoretical dipole and quadrupole contributions in the pre-edge region are presented separately in Fig. 10, together with the experimental curves. Note that the vertical axis is not in the same scale for the $\boldsymbol{\varepsilon}\|x,y$ and for the $\boldsymbol{\varepsilon}\|z$ components. The $\boldsymbol{k}$ vector components corresponding to the displayed curves are [0,0.383,0.924] for the $\boldsymbol{\varepsilon}\|x$ polarization, [0,0,1] for the $\boldsymbol{\varepsilon}\|y$ polarization and [0,1,0] for the $\boldsymbol{\varepsilon}\|z$ polarization. According to Eq. (2), corresponding partial spectral weights of quadrupole transitions are $0.147d_{xy}+0.853d_{xz}$ for the $\boldsymbol{\varepsilon}\|x$ polarization, while for the $\boldsymbol{\varepsilon}\|y$ and $\boldsymbol{\varepsilon}\|z$ polarizations the quadrupole component is a pure d_{yz}.

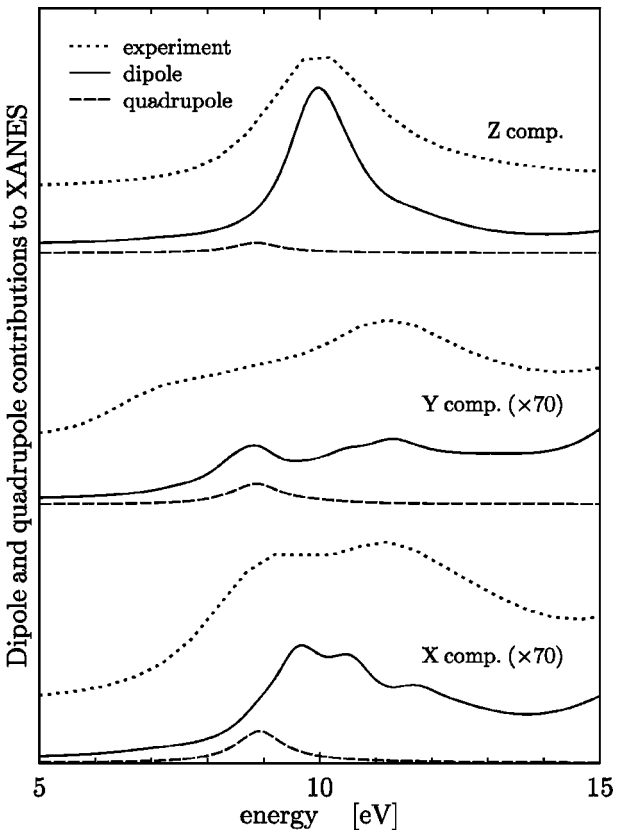

FIG. 10. Comparing calculated dipole and quadrupole contributions in the pre-edge region. The experiment is displayed for comparison as well. Note that again the $\boldsymbol{\varepsilon}\|x$ and $\boldsymbol{\varepsilon}\|y$ component intensities were multiplied by 70 (similarly as in Fig. 7). The $\boldsymbol{k}$ vector components are [0,0.383,0.924] for the $\boldsymbol{\varepsilon}\|x$ polarization, [0,0,1] for the $\boldsymbol{\varepsilon}\|y$ polarization, and [0,1,0] for the $\boldsymbol{\varepsilon}\|z$ polarization.

It can be seen from Fig. 10, that our calculation fails to reproduce the experiment in the pre-edge region for the $\boldsymbol{\varepsilon}\|x,y$ polarizations, even if quadrupole contributions are included. The most likely source of this disagreement is inadequacy of our non-self-consistent muffin-tin scattering potential. We checked that including quadrupole contributions in calculations *without* the core hole (cf. Sec. IV C and Fig. 7) does not improve the agreement with experiment either — hence, we do not display those results here.

Due to this failure, we did not try to verify by calculations our assumptions based on analysis of Fig. 9, namely that the dominant quadrupole components are d_{xy} and $d_{x^2-y^2}$. Nevertheless, few hints still could be collected from Fig. 10. First, our calculation agrees with the common experience that quadrupole contributions are likely to be most important at the low-energy tail of the prepeak.[14,35,42,53] Second, the middle panel of Fig. 10 supports the suggestion of Ref. 28 that the first peak in pre-edge structure in $\boldsymbol{\varepsilon}\|y$ spectrum contains a non-negligible quadrupole contribution — although the dipole component is still a bit larger. Note also that significant quadrupole nature of the low-energy side of the $\boldsymbol{\varepsilon}\|y$ prepeak could be guessed from the inset of Fig. 8 as well.

To conclude this section, we found a compelling evidence that quadrupole transitions contribute significantly to the details of the pre-edge structure for the $\boldsymbol{\varepsilon}\|x$ and even more for the $\boldsymbol{\varepsilon}\|y$ polarization. However, the precise ratio between di-

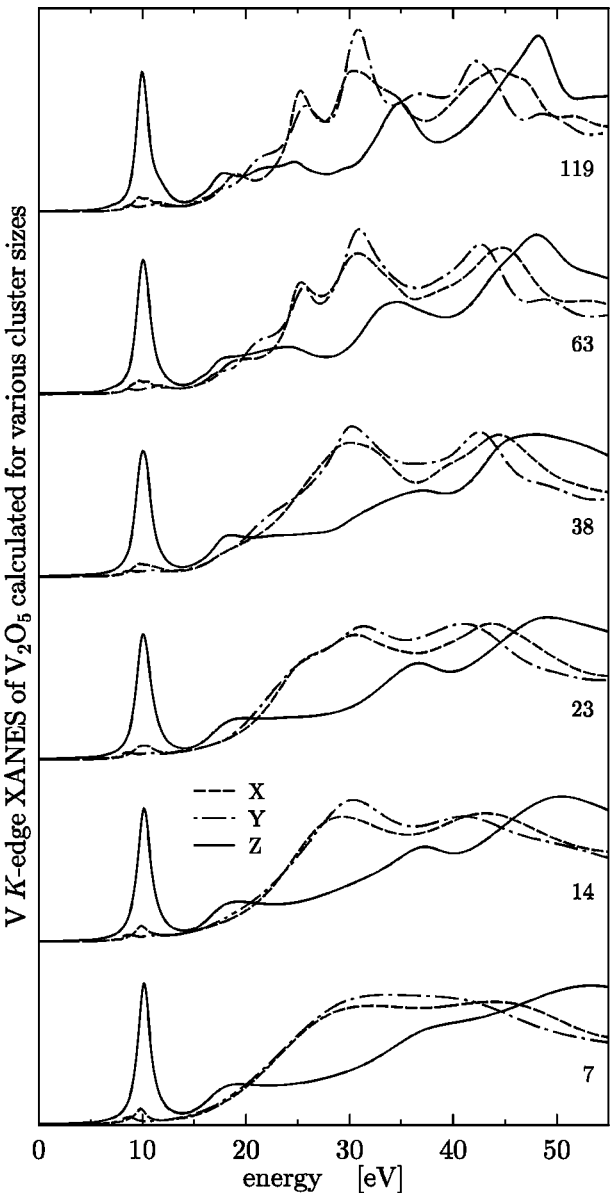

FIG. 11. Theoretical polarized XANES calculated for increasing cluster sizes. The numbers of atoms in respective clusters are indicated at each set of curves.

pole and quadrupole contributions as well as the symmetry type of the quadrupole transitions involved has yet to be quantified.

D. Cluster size effect

Theoretical V *K*-edge polarized XANES spectra for a few representative sizes of the clusters taken into account are displayed in Fig. 11. The first thing to notice is that the most characteristic features of the polarized spectra appear for as little as 7 atoms. This confirms in a systematic way earlier observations of Stizza *et al.*[31] and Kraizman *et al.*,[33] who perform their simulations for clusters of up to 7 or 19 atoms, respectively. Also the fact that spectra of V_2O_5 crystal, V_2O_5 xerogel, and $VOPO_4 \cdot 2H_2O$ gel are quite similar to each other in their general trends supports the conclusion that it is the nearest neighborhood of V atom, which is responsible for the gross spectral features (especially close to the edge).[28]

Let us take note that the cluster size convergence is not uniform: Main peak splittings at $\boldsymbol{\varepsilon} \| x$ and $\boldsymbol{\varepsilon} \| y$ appear at first for 23 atoms (peaks at 25 eV and 30 eV for $\boldsymbol{\varepsilon} \| x$ and at 25 eV and 31 eV for $\boldsymbol{\varepsilon} \| y$), then disappear at 38 atoms (only peaks at 30 eV for $\boldsymbol{\varepsilon} \| x$ and 31 eV for $\boldsymbol{\varepsilon} \| y$ are left) and definitely re-emerge at 63 atoms. This indicates that forming XANES peaks is a complex process and the association between particular spectral and geometrical features is not a straightforward one. Poumellec *et al.*[28] remarked that the splitting in question had not yet been explained by one-electron theory. Figure 11 demonstrates that this was due to the fact that the cluster size used by Stizza *et al.*[31] was simply too small to account for this. Use of more sophisticated exchange-correlation terms, as suggested in Ref. 28, is therefore, not necessary.

We found no significant changes between spectra obtained for clusters containing 63, 119, or even 255 atoms (the last spectrum not shown in Fig. 11) — not even at the pre-edge region. Hence, the failure of the theory to describe the pre-edge fine structure for $\boldsymbol{\varepsilon} \| x$ and $\boldsymbol{\varepsilon} \| y$ polarization cannot be due to cluster size effects.

The last remarkable thing to note is that the theoretical spectra converge more quickly with cluster size in the $\boldsymbol{\varepsilon} \| z$ polarization than in the $\boldsymbol{\varepsilon} \| x,y$ polarizations. This seems to be a consequence of a semilayered structure of V_2O_5: Due to the very short V-O_{van} bond length, the unoccupied states have rather molecular than solid-state character in the *z* direction.

E. Role of symmetry distortion

Departures of the arrangements of atoms around the central one from the perfect octahedral symmetry may have deep consequences for the shape of the absorption spectrum.[27] In order to study such effects in the case of a highly asymmetric V_2O_5 crystal, we calculate polarized spectra for artificial model structures, where selected deviations from the octahedral symmetry are relaxed.[37]

First, the V_2O_5 structure can be altered in such a way that the *horizontal* symmetry is recovered, i.e., the zig-zagged oxygen chains, which are approximately colinear with the *b* axis, as indicated in Fig. 2, are made straight. Note that such a model structure still is not isotropic in the *xy* plane. The original V_2O_5 structure can also be altered in such a way that the *vertical* symmetry is recovered, i.e. bipyramidal bases perpendicular to the *c* axis are made flat (cf. projection of the original V_2O_5 structure in Fig. 3). Positions of atoms in the model structures are summarized in Table III in fraction units.

Theoretical V *K*-edge XANES spectra for these two model compounds are displayed in Fig. 12. The calculations were performed for clusters containing 134 atoms (horizontal symmetry restored) or 148 atoms (vertical symmetry restored). The ''original V_2O_5'' spectrum, displayed for comparison, corresponds to 119 atoms in cluster. These cluster sizes ought to be fully sufficient (see Sec. IV D). Mattheiss potentials for the model compounds were constructed along directions appropriate for parameter set 1 of Sec. III A.

Due to a poor agreement of our theory with the experiment in the pre-edge region for $\boldsymbol{\varepsilon} \| x$ and $\boldsymbol{\varepsilon} \| y$ polarizations, our analysis is relevant mainly for larger photoelectron ener-

TABLE III. Positions of the vanadium atoms and of the three types of oxygens in model compounds derived from the original V_2O_5 crystal by restoring either the horizontal or the vertical symmetry. See Table I for the original V_2O_5 structure.

Atom	Wyckoff positions	x	y	z
	Horizontal symmetry restored			
V	(4f)	0.08333	0.25	0.8917
O_{van}	(4f)	0.08333	0.25	0.531
O_{ch}	(4f)	−0.08333	0.25	0.003
O_{bri}	(2a)	0.25	0.25	0.001
	Vertical symmetry restored			
V	(4f)	0.10118	0.25	0.000
O_{van}	(4f)	0.1043	0.25	0.500
O_{ch}	(4f)	−0.0689	0.25	0.000
O_{bri}	(2a)	0.25	0.25	0.000

gies. Hence we cannot compare directly with the analysis of Eyert and Höck,[37] as they cover just the lowest part of the conduction band. Rather, our investigation is complementary to theirs in this respect.

An interesting thing to notice in Fig. 12 is that recovering either vertical or horizontal symmetry changes the other polarization component as well, hinting thus possible significance of a *nonfocusing* multiple scattering[57,58] in respective energy regions (terms ''wide angle'' or ''type-2'' scattering have been used as well in the literature). That would be quite remarkable, as most studies indicate that only those scattering paths which are approximately colinear have to be taken indispensably into account by RS-MS theory.[59]

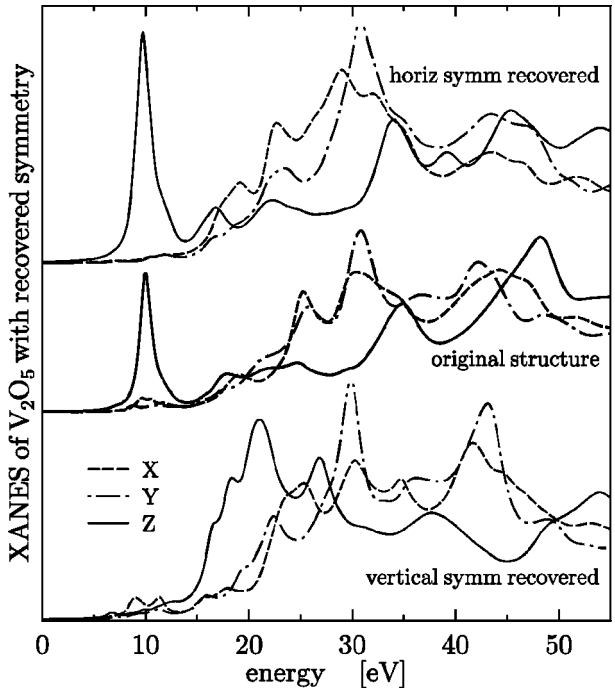

FIG. 12. Effect of restoring either horizontal symmetry (upper set of curves) or vertical symmetry (lower set of curves) in V_2O_5 crystal on the theoretical XANES spectrum. Polarized spectrum for the original V_2O_5 structure is displayed with thicker lines in the middle section.

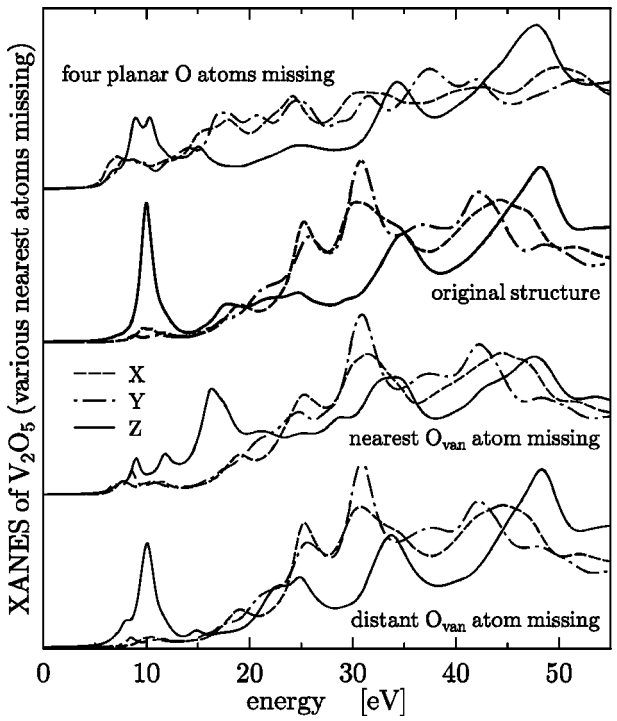

FIG. 13. Effect of removing specific nearest atoms from a large V_2O_5 cluster (119 atoms). The lowest spectra correspond to removing the distant vanadyl oxygen [labeled $O^1(2)$ in Fig. 1] — i.e., 118 atoms in cluster, the next triad of curves corresponds to removing the nearest vanadyl oxygen $O^1(1)$ (again 118 atoms in cluster), then come polarized spectra of the original V_2O_5 structure and uppermost curves correspond to removing four nearest planar oxygens (labeled in Fig. 1 as O^2 and O^3), leaving thus 115 atoms in the cluster.

The $\boldsymbol{\varepsilon}\|z$ spectrum remains relatively unchanged if the horizontal symmetry is restored but crucially depends on the presence of vertical displacements (even beyond the preedge region). The horizontal components $\boldsymbol{\varepsilon}\|x,y$, if viewed separately, are not changed dramatically by either symmetry restoration. However, their mutual positions (polarization distinction) depends quite a lot on the absence or presence of either vertical or horizontal symmetry. As a whole, the $\boldsymbol{\varepsilon}\|x,y$ components seem to be much less dependent on the (deficient) symmetry of the V_2O_5 crystal than the $\boldsymbol{\varepsilon}\|z$ component.

F. Origin of peaks — effects of particular atoms

In order to learn more about the importance of particular atoms for specific XANES features, we calculated model spectra for large V_2O_5 clusters, with various nearest-oxygen atoms missing. In Fig. 13, we present theoretical polarized spectra for a cluster with the four ''planar'' oxygens missing (three O_{ch} and one O_{bri} atoms, labeled O^2 and O^3 in Fig. 1), for another cluster where just the nearest vanadyl oxygen O_{van} is missing [labeled $O^1(1)$ in Fig. 1], and finally for a cluster with only the *distant* vanadyl oxygen removed [labeled $O^1(2)$ in Fig. 1].

We can observe that the $\boldsymbol{\varepsilon}\|z$ component remains more-or-less intact by any changes in the nearest vanadium neighborhood for $E>30$ eV. Moreover, even the near-edge region of $\boldsymbol{\varepsilon}\|z$ is little affected by presence or absence of the nearest four planar oxygens. The same is even more valid for the

distant O_{van} atom: The $\boldsymbol{\varepsilon}\|z$ spectrum varies only slightly if this atom is removed from a large cluster, the changes being almost exclusively restricted to the ''critical area'' around 20 eV. On the contrary, the presence of the nearest O_{van} is *crucial* for the occurrence of the $\boldsymbol{\varepsilon}\|z$ prepeak.

The sensitivity of $\boldsymbol{\varepsilon}\|x$ and $\boldsymbol{\varepsilon}\|y$ spectra to presence or absence of nearest atoms offers much less surprising features: The $\boldsymbol{\varepsilon}\|x,y$ components change totally in the *whole energy range* if nearest planar oxygens are removed (uppermost section of Fig. 13). Presence or absence of any of the apical vanadyl oxygens O_{van} is not essential for $\boldsymbol{\varepsilon}\|x$ and $\boldsymbol{\varepsilon}\|y$ spectra except for the pre-edge region.

Thus, by analyzing curves in Fig. 13, we can draw a conclusion that the distinct prepeak in the $\boldsymbol{\varepsilon}\|z$ spectrum is determined almost exclusively by the nearest vanadyl oxygen — as though the rest of the cluster acted just like a mirror, reflecting the outgoing electron back to the center and enhancing the effect of the O_{van} atom in question. To explore this suggestion deeper, we proceed the other way now: We calculate XANES spectra for very small model clusters, which contain just few atoms concerned.

The results are shown in Fig. 14. The curves are distinguished by inset symbolic drawings. The largest cluster considered here contains just 7 atoms and consists of a vertically distorted square bipyramid. To highlight the role of the vanadyl oxygens O_{van}, the model clusters were made completely symmetric in the xy plane: The four planar oxygens lie in the same plane as the V atom, at the corners of a square. The distance of all the planar oxygens from the central V is 1.89 Å for these model structures. There is thus no difference between the $\boldsymbol{\varepsilon}\|x$ and $\boldsymbol{\varepsilon}\|y$ spectra. The vanadyl oxygens are put in the apices of the bipyramid.

The uppermost pair of curves corresponds to the ''real'' V_2O_5 cluster — the apical oxygens are placed at distances 1.58 and 2.79 Å from the V atom, respectively. The pre-peak in $\boldsymbol{\varepsilon}\|z$ is well defined. Next comes a *symmetric* bipyramid (both apical oxygens are put 1.58 Å from the center). The prepeak completely disappears for this centrosymmetric environment. The two following pairs represent simple pyramids (6 atoms in cluster). The prepeak is present only for the 1.58-Å distance of the apical oxygen — it vanishes if this length is increased to 2.79 Å . A similar situation occurs if the planar oxygens are left out, i.e. we have just three atoms in the clusters (following two pairs of curves). And finally this picture holds also if we take into account just the central V atom and one oxygen (the lowermost pairs in Fig. 14): The prepeak is absent for the longer V–O distance.

Thus we can draw a conclusion: The characteristic prepeak in the $\boldsymbol{\varepsilon}\|z$ component of the V *K*-edge XANES spectrum of V_2O_5 is concurrently caused by the breaking of the central symmetry *and* by the presence of the short $V\text{–}O_{van}$ bond. We actually scanned a broad range of $V\text{–}O_{van}$ distances, calculating XANES spectra for a set of model simple pyramids (6 atoms in cluster). We found that if the nearest vanadyl oxygen distance (1.58 Å) is gradually increased, the pre-peak shrinks and practically disappears if this distance reaches $\sim$2.2 Å .

Our accentuation of the shortest $V\text{–}O_{van}$ distance is consistent with deductions made earlier by other methods. E.g. Wong *et al.*[27] used semiquantitative arguments to explain the trends in the dependence of prepeak height on few short

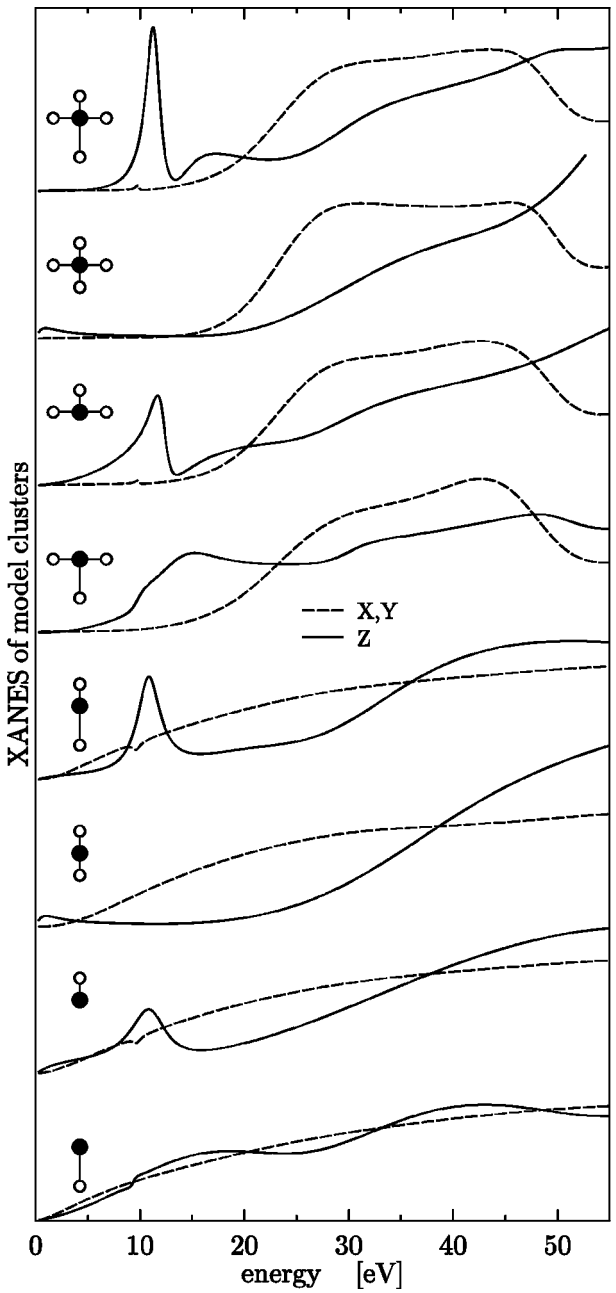

FIG. 14. Theoretical spectra of small model clusters (containing from 2 to 7 atoms) which simulate the nearest neighborhood of V in V_2O_5. Each model structure is schematically identified by the inset drawing. See the text for a detailed description.

bond lengths, and found that the contribution of the shortest bond is about three times as high as one would expect from the fractions of the short V–O bonds to the total number of V-ligand bonds in the compounds under consideration. The role of $V\text{–}O_{van}$ bond lengths asymmetry was stressed also for $VOPO_4\cdot 2H_2O$ (Ref. 35). In the case of intercalated $Li_xV_2O_5$ compounds, theoretical simulations of Lemoigno *et al.*[60] indicate that displacements of apical oxygens play an essential role in explaining changes observed in the experimental V *K*-edge spectra of intercalates.

The interpretation of higher-energy features is more complicated. The composite peak at 19–23 eV in the $\boldsymbol{\varepsilon}\|z$ experimental spectrum seems to be quite sensitive to the presence of the distant O_{van} atom — cf. lowest set of curves in Fig. 13.

However, a faint peak appears here even without it (see the third pair of curves from the top in Fig. 14). The role of the distant O_{van} was stressed in this context also by Stizza *et al.*,[31] although they analyzed XANES of $V_2O_5 \cdot 1.6H_2O$ gel and therefore, their results cannot be directly applied to this case.

Poumellec *et al.*[28] attribute the main peaks at 24–31 eV in $\boldsymbol{\varepsilon} \| x$ and $\boldsymbol{\varepsilon} \| y$ polarizations to transitions to states derived from atomiclike *p* states of the central V, neighboring O and neighboring V atoms. This corresponds to 14 atoms in cluster. Figure 11 reveals indeed, that for this cluster size a well-defined broad peak around 30 eV emerges. However, as discussed in Sec. IV D, more distant shells are also important here and, in fact, they cause the splitting of this peak into two.

As already noted above, a remarkable feature of the $\boldsymbol{\varepsilon} \| z$ theoretical polarization component is that it does not change significantly for $E > 30$ eV if either nearest apical or nearest-planar oxygens are removed (Fig. 13). This disputes the proposal that the structures at 35 and 48 eV of the $\boldsymbol{\varepsilon} \| z$ spectrum are representative for the 1.58-Å bond distance.[28]

As a whole, it seems that the spectral peaks at $E > 15$ eV arise due to quite complex scattering processes and it is not at all clear which atoms and/or scattering paths are essential for their generation. There seems to be a compelling need to develop an intuitively plausible scheme to connect specific geometrical and spectral features in a more conclusive way.

V. CONCLUSIONS

We presented experimental and theoretical polarized V *K*-edge spectra of V_2O_5. Our transmission-mode collected spectra agree with electron-yield detection spectra of Poumellec *et al.*,[28] with the exception of the inverted ratio of intensities of subpeaks at 19 eV and 23 eV in the $\boldsymbol{\varepsilon} \| z$ polarization. We found that our non-self-consistent muffin-tin RS-MS calculation can account for the basic polarizations trends and for peak heights and positions of the experimental spectra. Differences between experiment and theory in some distinct details are evident for the polarized spectra, however. Those differences are not so apparent when comparing unpolarized spectra—only polarized spectra provide an ''acid test'' for the theory.

Our calculations, either with or without the core hole, do not reproduce correctly the pre-edge structure in the $\boldsymbol{\varepsilon} \| x$ and $\boldsymbol{\varepsilon} \| y$ polarizations, even if quadrupole contributions are taken into account. By comparing theoretical spectra obtained for muffin-tin potentials constructed in different ways, we infer that non-muffin-tin effects may be important in XANES of V_2O_5 — especially in the pre-edge region.

By analyzing polarization dependence of the experimental spectra alone, we found evidence that the details of the pre-edge fine structure for the $\boldsymbol{\varepsilon} \| x,y$ polarization are visibly influenced by quadrupole transitions. Our data suggest that these quadrupole contributions could arise predominantly from the d_{xy} and $d_{x^2-y^2}$ partial spectra components.

We tried to identify origins of particular spectral peaks. We demonstrated that the cluster size convergence of polarized XANES spectra of V_2O_5 is not uniform and it depends on the polarization. By calculating XANES for model compounds, we argue that deviations of the V_2O_5 crystal structure from the horizontal symmetry are much less significant for the shape of the spectrum than deviations from the vertical symmetry. Presence of the nearest O_{van} atom is necessary for generating the distinct pre-peak in $\boldsymbol{\varepsilon} \| z$ component. For existence of this feature, both *short bond length* and *asymmetry* are crucial. The high-energy tail of the $\boldsymbol{\varepsilon} \| z$ spectrum ($E > 30$ eV) seems to be generated by long-range scattering — it does not depend on the presence or absence of the nearest neighbors of the central V.

ACKNOWLEDGMENTS

The theoretical work was supported by Grant No. 202/97/0566 of the Grant Agency of the Czech Republic. The experimental work was supported by Hamburger Synchrotronstrahlungslabor HASYLAB (Project No. II-95-67). Use of the CRYSTIN database was funded by Grant No. 203/99/0067 of the Grant Agency of the Czech Republic.

[1] P. J. Durham, J. B. Pendry, and C. H. Hodges, Solid State Commun. **38**, 159 (1981).
[2] D. D. Vvedensky, in *Unoccupied Electron States*, edited by J. C. Fuggle and J. E. Inglesfield (Springer, Berlin, 1992), p.139.
[3] J. E. Müller and J. W. Wilkins, Phys. Rev. **29**, 4331 (1984).
[4] F. W. Kutzler, C. R. Natoli, D. K. Misemer, S. Doniach and K. O. Hodgson, J. Chem. Phys. **73**, 3274 (1980).
[5] J. Stöhr, *NEXAFS Spectroscopy* (Springer, Berlin, 1992).
[6] P. J. W. Weijs *et al.*, Phys. Rev. B **41**, 11 899 (1990).
[7] E. Tamura, J. van Elk, M. Fröba, and J. Wong, Phys. Rev. Lett. **74**, 4899 (1995).
[8] O. Šipr, P. Machek, A. Šimůnek, J. Vackář, and J. Horák, Phys. Rev. B **56**, 13 151 (1997).
[9] J. Schwitalla and H. Ebert, Phys. Rev. Lett. **80**, 4586 (1998).
[10] J. Chaboy and S. Quartieri, Phys. Rev. B **52**, 6349 (1995).
[11] A. L. Ankudinov and J. J. Rehr, J. Phys. IV **7** Colloq., C2 C2-121 (1997).
[12] D. L. Foulis, R. F. Pettifer, and P. Sherwood, Europhys. Lett. **29**, 647 (1995).
[13] Y. Joly, J. Phys. IV **7** Colloq., C2 C2-111 (1997).
[14] Y. Joly, D. Cabaret, H. Renevier, and C. R. Natoli, Phys. Rev. Lett. **82**, 2398 (1999).
[15] T. Huhne and H. Ebert, Solid State Commun. **109**, 577 (1999).
[16] F. M. F. de Groot, J. C. Fuggle, B. T. Thole, and G. A. Sawatzky, Phys. Rev. B **41**, 928 (1990); **42**, 5459 (1990).
[17] A. V. Soldatov, T. S. Ivanchenko, A. P. Kovtun, S. Della Longa, and A. Bianconi, Phys. Rev. B **52**, 11 757 (1995).
[18] A. L. Ankudinov, B. Ravel, J. J. Rehr, and S. D. Conradson, Phys. Rev. B **58**, 7565 (1998).
[19] O. Šipr, F. Rocca, and G. Dalba, J. Synchrotron Rad. **6**, 770 (1999).
[20] P. Kitzler, Phys. Rev. B **46**, 10 540 (1992).
[21] Z. Y. Wu, S. Gota, F. Jollet, M. Pollak, M. Gautier-Soyer, and C. R. Natoli, Phys. Rev. B **55**, 2570 (1997).

[22] Y. Jeanne-Rose, B. Poumellec, and Y. Aïfa, J. Phys. IV **7** Colloq. C2, C2-221 (1997).
[23] A. L. Ankudinov, S. D. Conradson, J. Mustre de Leon, and J. J. Rehr, Phys. Rev. B **57**, 7518 (1998).
[24] D. A. McKeown, Phys. Rev. B **45**, 2648 (1992).
[25] Z. Y. Wu, G. Ouvrard, P. Moreau, and C. R. Natoli, Phys. Rev. B **55**, 9508 (1997).
[26] F. Farges, G. E. Brown, Jr., and J. J. Rehr, Phys. Rev. B **56**, 1809 (1997).
[27] J. Wong, F. W. Lytle, R. P. Messmer, and D. H. Maylotte, Phys. Rev. B **30**, 5596 (1984).
[28] B. Poumellec, R. Cortes, C. Sanchez, J. Berthon, and C. Fretigny, J. Phys. Chem. Solids **54**, 751 (1993).
[29] R. M. Abdel-Latif, Physica B **254**, 273 (1998).
[30] S. Stizza, M. Benfatto, I. Davoli, G. Mancini, A. Marcelli, A. Bianconi, M. Tomellini, and J. Garcia, J. Phys. (France) **46**, Colloq. C8, 255 (1985).
[31] S. Stizza, M. Benfatto, A. Bianconi, J. Garcia, G. Mancini, and C. R. Natoli, J. Phys. (France) **47**, Colloq. C8, 691 (1986).
[32] V. M. Cherkashenko, V. E. Dolgikh, and V. L. Volkov, Fiz. Tverd. Tela (Leningrad) **30**, 386 (1988) [Sov. Phys. Solid State **30**, 220 (1988)].
[33] V. L. Kraizman, A. A. Novakovich, V. I. Popov, V. M. Cherkashenko, and E. Z. Kurmaev, Ukr. Fiz. (Russ. Ed.) **35**, 915 (1990).
[34] V. L. Kraizman and A. A. Novakovich, in *X-Ray Absorption Fine Structure*, Proceedings of the XAFS VI Conference, York, 1990, edited by S. S. Hasnain (Ellis Horwood, Chichester, 1991), p. 70.
[35] B. Poumellec, V. Kraizman, Y. Aifa, R. Cortes, A. Novakovich, and R. Vedrinskii, Phys. Rev. B **58**, 6133 (1998).
[36] E. Goering, O. Müller, M. Klemm, M. L. denBoer, and S. Horn, Philos. Mag. B **75**, 229 (1997).
[37] V. Eyert and K.-H. Höck, Phys. Rev. B **57**, 12 727 (1998).
[38] A. Šimůnek, O. Šipr, S. Bocharov, D. Heumann, and G. Dräger, Phys. Rev. B **56**, 12 232 (1997).
[39] S. Bocharov, G. Dräger, D. Heumann, A. Šimůnek and O. Šipr, Phys. Rev. B **58**, 7668 (1998).
[40] C. Brouder, J. Phys.: Condens. Matter **2**, 701 (1990).
[41] J. E. Hahn, R. A. Scott, K. O. Hodgson, S. Doniach, S. R. Desjardins, and E. I. Solomon, Chem. Phys. Lett. **88**, 595 (1982).
[42] T. Uozumi, K. Okada, A. Kotani, O. Durmeyer, J. P. Kappler, E. Beaurepaire, and J. C. Parlebas, Europhys. Lett. **18**, 85 (1992).
[43] G. Dräger, R. Frahm, G. Materlik, and O. Brümmer, Phys. Status Solidi B **146**, 287 (1988).
[44] D. Heumann, G. Dräger, and S. Bocharov, J. Phys. IV **7**, Colloq. C2, 481 (1997).
[45] D. D. Vvedensky, D. K. Saldin, and J. B. Pendry, Comput. Phys. Commun. **40**, 421 (1986).
[46] G. Bergerhoff, R. Hundt, R. Sievers, and I. D. Brown, J. Chem. Inf. Comput. Sci. **23**, 66 (1983).
[47] M. Dušek, PICTUR, Institute of Physics AS CR, Praha, 1994.
[48] L. F. Mattheiss, Phys. Rev. A **133**, A1399 (1964); **134**, A970 (1964).
[49] J. Vackář, LDAT, Institute of Physics AS CR, Praha, 1986.
[50] See e.g. W. E. Pickett, Comput. Phys. Rep. **9**, 115 (1989).
[51] W. Kohn and L. J. Sham, Phys. Rev. **140**, A1133 (1965).
[52] C. Li, M. Pompa, A. Congiu-Castellano, S. Della Longa, and A. Bianconi, Physica C **175**, 369 (1990).
[53] R. V. Vedrinskii, V. L. Kraizman, A. A. Novakovich, Ph. V. Demekhin, and S. V. Urazhdin, J. Phys.: Condens. Matter **10**, 9561 (1998).
[54] F. Al Shamma, M. Abbate, and J. C. Fuggle, in *Unoccupied Electron States*, edited by J. C. Fuggle and J. E. Inglesfield (Springer, Berlin, 1992), p. 347.
[55] N. Kosugi, T. Yokoyama, K. Asakura, and H. Kuroda, Chem. Phys. **91**, 249 (1984); T. Yokoyama, N. Kosugi, and H. Kuroda, *ibid.* **103**, 101 (1986).
[56] I. M. Curelaru, E. Suoninen, and E. Minni, J. Chem. Phys. **78**, 2262 (1983).
[57] G. Bunker and E. A. Stern, Phys. Rev. Lett. **52**, 1990 (1984).
[58] D. D. Vvedensky and J. B. Pendry, Surf. Sci. **162**, 903 (1985).
[59] L. A. Bugaev, Ph. Ildefonse, A.-M. Flank, A. P. Sokolenko, and H. V. Dmitrienko, J. Phys.: Condens. Matter **10**, 5463 (1998).
[60] F. Lemoigno, E. Prouzet, Z. Y. Wu, P. Gressier, and G. Ouvrard, J. Phys. IV **7**, Colloq. C2, 263 (1997).